M-AM-Sym II-1

STRUCTURE OF ADENOVIRUS BY CRYSTALLOGRAPHY AND ELECTRON MICROSCOPY

Roger M. Burnett
The Wistar Institute, Philadelphia, PA 19104

Adenovirus is a mammalian virus with a characteristic icosahedral non-enveloped virion of diameter 1000 Å and 300 Å fibers projecting from its 12 vertices. The type 2 virion contains approximately 2700 polypeptides, from at least 10 different protein species, and 35,937 base pairs of linear double-stranded DNA. Hexon, the major coat protein, is present in 240 trimers accounting for 62% of the particle mass of 150×10^6 Daltons. The size of the particle has required a novel combination of two imaging methods for its structural solution.

The crystal structure of the type 2 hexon polypeptide of 967 residues has been determined and refined at 2.9 Å resolution with both conventional least-squares and molecular dynamics methods. Hexon has a pseudo-hexagonal base containing three sets of two 8-stranded β-barrels topologically related to each other and to all known viral coat barrels. The triangular top is formed by loops, arising from the basal barrels, that intertwine to form the protuberances visible on the viral surface.

The architecture of the virion has been determined using the known hexon structure to interpret EM images, both qualitatively and quantitatively. Image analysis was used to identify, and then average, similar images of negatively stained capsid fragments from conventional and scanning transmission EM. The former established relative hexon orientations at ~50 Å resolution and led to a model for the capsid. The latter provided 18 Å images that, upon subtraction of the crystallographic hexon images, revealed a small capsid-cementing protein. A 3-dimensional image reconstruction of the entire virion using cryo-electron microscopy at ~30 Å resolution indicates revisions to the capsid model, reveals the fibers and other capsid components, and shows order in the DNA/protein complex in the core.

Supported by NIH (AI-17270) and NSF (DMB 89-96195).

M-AM-Sym II-2

THE STRUCTURE OF HIV CORE BY ELECTRON MICROSCOPE TOMOGRAPHY

Stefan Höglund[1], Lars-Göran Öfverstedt[1], Asa Nilsson[1], Pär Lundquist[1], Hans Gelderblom[2], Muhsin Özel[2], Thorsten Winkel[2], and Ulf Skoglund[3]

[1]Department of Biochemistry, Biomedical Center, Box 576, S-751 23 Uppsala, Sweden

[2]Institute of Virology, Robert-Koch Institute of the Federal Health Administration, D-1000 Berlin 65, Germany

[3]Department of Molecular Genetics, Karolinska Institutet, Box 60400, S-104 01 Stockholm, Sweden

Single, about 80 nm thick, ultrathin plastic sections of embedded HIV-1 infected H9 cells have been reconstructed in three dimensions at 5 nm resolution by electron microscope tomography according to the filtered back-projection principle, The whole virus has a diameter of about 150 nm. The objective of the study was to characterize the core of the virus to visualize the internal assembly of late states of maturing HIV-1 and to provide well defined measures that will aid in defining its maturation state. The core consists of two ribonucleo-protein fibers (with identical RNA strands) folded into a flattened, hollow cone with one end being wide and flexible and the other narrow and compact. The narrow end reaches the envelope via a 8-10 nm wide core-envelope-link (CEL) structure that could be important for the morphogenesis of the virus by serving as a template during the assembly and maturation. Thus the CEL could be a potential prospective for drugs and subunit vaccines, interfering with viral maturation and infection.

M-AM-Sym II-3

TIME-RESOLVED MACROMOLECULAR CRYSTALLOGRAPHY: PROJECTS AND RESULTS

Keith Moffat
Department of Biochemistry and Molecular Biology
The University of Chicago
Chicago, IL 60637

Changes in tertiary structure lie at the heart of all biochemical processes at the molecular level. A complete understanding of, for example, enzyme catalysis, ligand binding and release by hemoglobin, calmodulin, and immuno-globulins, photocycling in sensory systems, and protein unfolding/refolding requires elucidation of intermediate structures and not just stable reactants and products. However, such intermediates are generally short-lived and difficult to study by conventional techniques of structure determination using, for example, x-ray crystallography.

With the advent of extremely intense, polychromatic synchrotron x-ray sources, x-ray exposures on strongly scattering protein crystals have been reduced to the millisecond time range and even, in one unusual case, to the 100 picosecond time range.

A time-resolved x-ray experiment then has three components: reaction initiation, uniformly and rapidly throughout the crystal; reaction monitoring through change in real time of the x-ray intensities; and data analysis to extract the underlying changes in structure.

The principles will be discussed, together with recent experimental results.

M-Am-Sym II-4

THREE-DIMENSIONAL MAP OF *PhoE* PORIN AT 3.5Å BASED ON ELECTRON CRYSTALLOGRAPHY

Bing K. Jap, Peter Walian, Kalle Gehring and Thomas Earnest

PhoE porin is a member of a family of pore forming proteins that are found in the outer membrane of Gram-negative bacteria. PhoE porin has been shown to have some selectivity for anionic and phosphate containing compounds, and, like other porins, it acts as receptors for various bacterial phages. We have analyzed 70 diffraction patterns of PhoE porin at tilt angles ranging from 0 to about 60 degrees from the membrane plane. We have also obtained high resolution images with the same range of tilt angles. Data from 30 images, from tilted and untilted samples, were processed to a resolution of about 3.5Å. The structure factor amplitude of the images were replaced by those that can be obtained more accurately from diffraction patterns. The phases were refined and extended to 3.5Å resolution by taking advantage of the use of non-crystallographic symmetry and the use of density modification techniques. The three-dimensional (3-D) map was generated from the combined structure factor amplitudes and refined phases by Fourier transformation.

The 3-D map at this resolution shows that porin consists of a trimer of elliptical, β-sheet cylinders. Each elliptical cylinder has a major axis of ~ 38Å and a minor axis of ~ 28Å as measured from the center of the β-sheet wall. The cylinder wall is formed by β-sheet having the major fraction of β-strands tilted by 35 degrees from the membrane normal. There is an internal structure that forms a layer that is located within the elliptical cylindrical structure and is furthest away from the three-fold axis. This internal layer defines the channel structure itself. The map clearly shows that the trimeric cylindrical structure does not merge to a single pore as reported for OmpF porin and for porin from *Rhodopseudomonas capsulata*. At the center of the three-fold symmetry of PhoE porin trimer, there is a low density that extends from the extracellular surface to about the center of the membrane. This low density domain, which faces the cell surface, has been proposed to contain lipopolysaccharide as a part of the structure of the protein in the native state. The channel is not straight and is consistent with the data obtained from our earlier 3-D model of negatively stained PhoE samples at 20Å resolution.

M-AM-F1

ATP-DEPENDENT POTASSIUM CHANNELS IN RABBIT AND BOVINE AIRWAY SMOOTH MUSCLE. Mei Lin Collier, Charles HC Twort, and Jeremy PT Ward, (Intro. by Michael J Mulvany). Division of Medicine, U.M.D.S., St Thomas' Hospital, London SE1 7EH, U.K.

ATP-dependent potassium channels have been implicated as the site of action for hyperpolarizing vasodilators, in particular the class of compounds known as potassium channel openers (Standen et al., *Science* 1989:245,177-180). These compounds have also been shown to relax airway smooth muscle (Allen et al., *Br.J.Pharmacol.*, 1986:89:395-405), but so far there is no electrophysiological evidence that ATP-dependent potassium channels are present in this tissue, and only a few reports for vascular smooth muscle.

Airway smooth muscle cells were freshly isolated with papain and collagenase from rabbit and bovine trachealis. Channel activity was investigated using the inside-out configuration of the patch clamp technique. The pipette solution contained (in mM) 50 KCl, 80 NaCl, and 5 HEPES; and that of the bath 140 KCl, 5 EGTA, 0.5 KH_2PO_4. K_2ATP, BRL38227 (the L-enantiomer of cromakalim), and glibenclamide were added to the bath solution. Recordings were made at room temperature, filtered at 1kHz and sampled at 4kHz.

Most membrane patches exhibited a small channel in the absence of ATP, which had a reversal potential corresponding to that of the K equilibrium potential. The channel had a unitary conductance of 38.5±1.3 pS in membranes from rabbit tissue, and 30.2±6.7 pS in bovine tissue. Open state probability was normally low (less than 0.2), and only slightly voltage sensitive. ATP (2 mM) abolished the current, but subsequent addition of BRL38227 (1μM) increased open state probability with no change in conductance. Glibenclamide (10μM) resulted in partial blockade. Open and closed-time histograms were best fitted by two exponential terms. Without ATP the time constants were approximately 8 and 124 ms for the open-time histogram, and 1 and 54 ms for the closed-time histogram. These results are similar to those described for ATP-dependent K channels in both heart and vascular smooth muscle.

We thank SmithKline Beecham for the gift of BRL38227.

M-AM-F2

NUCLEOTIDE DIPHOSPHATES ENHANCE NICORANDIL-MEDIATED ACTIVATION OF ATP-SENSITIVE K CHANNELS IN GUINEA-PIG VENTRICULAR MYOCYTES. W.K. Shen, R.T. Tung, M.M. Machulda, Y. Kurachi, Division of Cardiovascular Diseases, Department of Medicine, Mayo Clinic, Rochester, MN 55905

Nicorandil (2-nicotinamidoethyl nitrate) hyperpolarizes smooth muscle and cardiac cell membrane potentials. This is the electrophysiologic basis for the therapeutic applications of nicorandil. In the whole-cell and the cell-attached patch conditions, 10-100 μM nicorandil effectively activate ATP-sensitive K channels (K_{ATP}) in the presence of mM concentrations of intracellular ATP. However, in the inside-out patch condition, nicorandil is unable to activate K_{ATP} when [ATP] is in the mM range. To elucidate the possible intracellular factors underlying nicorandil-mediated K_{ATP} activation, we examined the effects of nucleotide diphosphates (NDPs=ADP, GDP, and UDP) in the regulation of K_{ATP} by using isolated inside-out patches from guinea-pig ventricular myocytes. Upon formation of inside-out patches in ATP-free internal solution, K_{ATP} openings appeared vigorously and then decayed spontaneously (run-down), probably due to channel dephosphorylation. We observed the following: (1) Nicorandil (10 μM-1mM) could not activate K_{ATP} after run-down. (2) Nicorandil mildly activated K_{ATP} in solution containing 0.1 mM ATP; the activation of K_{ATP} was completely suppressed at higher [ATP]. (3) NDPs could activate K_{ATP} after run-down. (4) NDPs-induced K_{ATP} openings were completely inhibited by high concentrations of ATP (>0.5 mM). (5) Nicorandil (300 μM) effectively activated K_{ATP} even in high concentrations of ATP when NDPs(500 μM) were present. These observations suggest that under physiological conditions, where [ATP] is in the mM range, NDPs may be required in the nicorandil-mediated activation of K_{ATP}.

M-AM-F3

ANOXIA OPENS ATP REGULATED K CHANNELS IN GUINEA PIG CARDIOCYTES

K. Benndorf, M. Friedrich, G. Bollmann, C. Hansen, Hj. Hirche (Intro. by P.F. Cranefield) Institut für Vegetative Physiologie, Universität Köln, Robert-Koch-Str. 39, 5000 Köln 41, FRG.

In isolated cardiocytes, metabolic inhibitors or hypoxic conditions substantially shorten action potentials by inducing a large time-independent K current. During metabolic blockade, this current flows through ATP-regulated K channels which open after sufficient ATP depletion. We studied the effect of anoxia ($pO_2 < 0.1$ torr) on guinea pig cardiocytes in cell-attached patches to identify the type of single K channels which open. Using 150 mmol/l KCl in the pipette and a Tyrode solution with 10.8 mmol/l KCl in the bath, inward K currents were recorded at negative potentials. After periods of 5-60 minutes of anoxia, the open probability (P_o) of inward rectifier channels decreased to 0-10% and openings of one to four voltage-independent 83 pS channels developed (T=35 °C). Within one minute, P_o of this type of channel reached a steady state value between 0.6 and 0.95. At maximum P_o, open and closed time histograms, evaluated at voltages between -85 and -45 mV, were dominated by fast exponentials with time constants of 0.46 ± 0.20 msec and 0.53 ± 0.23 msec (mean±SD), respectively. The reversal potential of the unitary currents was determined to be -2 mV with 150 mmol/l K^+ in the pipette and -67 mV with 10.8 mmol/l K^+ in the pipette, indicating that the channels were highly selective for K^+. Voltage ramp experiments showed that single channel currents were slightly rectifying in an inward direction. Glibenclamide (1 μmol/l), administered under anoxic conditions, reversibly blocked the anoxia-induced channels. At 5.4 mmol/l K^+ in the pipette, anoxia-induced unitary currents were small (0.7 ± 0.1 pA at 0 mV). A correspondingly low slope conductance (8 pS) was obtained by noise analysis of whole cell current.

Conclusion: Anoxia opens ATP regulated K channels in isolated cardiocytes after intracellular ATP levels have sufficiently dropped down. At physiological levels of $[K^+]_o$, the single channel conductance is considerably reduced by a fast block, most likely by intracellular Mg^{++} and Na^+.

M-AM-F-4

LYSOPHOSPHOLIPIDS MODULATE THE K(ATP) CHANNEL.

G.T. Eddlestone and S. Ciani, Dept. of Physiology, UCLA School of Medicine, Los Angeles, Ca. 90024.

The action of phospholipase A_2 on membrane phospholipids yields both a fatty acid and a lysophospholipid (lysoPL). While fatty acids have been demonstrated to influence the activity of several channel types, the role of lysoPL's has not been extensively investigated. The ATP-sensitive K channel is present in many different tissues where it may fulfill an important role in the control of membrane potential. In a patch clamp study using the HIT insulin secreting cell line, we have assessed the effects of exogenous lysoPL's on K(ATP) channel activity, since particular lysoPL's, lysophosphatidylinositol (lysoPI) and lysophosphatidylcholine (lysoPC), initiate insulin secretion from islets of Langerhans while others, lysophosphatidylethanolamine (lysoPE) and lysophosphatidylserine (lysoPS), do not. In cell-attached patch experiments addition of lysoPC or lysoPI (10-1000 ng/ml) dose-dependently provoked closure of the K(ATP) channel, cell depolarization and initiation of action potentials; this effect commenced within 2 minutes of addition and was fully reversible within 5 minutes of removal. In contrast, lysoPE or lysoPS at concentrations of up to 10 ug/ml failed to effect any consistent change in channel activity. These data indicate a specific role for lysoPC and lysoPI in the modulation of K(ATP) channel activity. In the inside-out patch with 10 uM ATP and 50 uM GTP in the bath, lysoPC and lysoPI (10-1000 ng/ml) reversibly blocked the K(ATP) channel while lysoPS and lysoPE did not. These latter data indicate that the effects of lysoPC and lysoPI on the K(ATP) channel are mediated within the membrane and it may be suggested that the interaction is directly with the channel itself. The ability of these compounds to cause cell depolarization explains, at least in part, their role as initiators of insulin release; since this pathway is likely to be active in other cell types which manifest the K(ATP) channel, it is expected that specific lysoPL's will similarly affect the membrane potential and consequently the voltage dependent behavior of these cells. *(GTE supported by NIH grant # DK39652-01).*

M-AM-F5

ALTERATIONS IN VOLTAGE-GATED K^+ CURRENTS ASSOCIATED WITH AN EARLY STAGE IN THE DIFFERENTIATION OF HEMATOPOIETIC MYELOBLASTS

L. Lu, D. Markakis, W.B. Guggino* and R.W. Craig. Department of Physiology, Johns Hopkins School of Medicine, Baltimore, MD 21205

We have identified a novel K^+ current in the ML-1 human myeloblastic leukemia cell line. The K^+ current is activated by depolarization of the membrane potential from a holding potential of -100 mV to more than -60 mV (n=22). Inactivation of the current is also voltage-dependent, with a time constant (τ_i) of 900 ms at 0 mV. Tail current analysis showed that the reversal potential of the current is shifted from -90 to -20 mV (n=4) when extracellular K^+ concentration is increased from 2 to 60 mM. The current is inhibited by 4-Aminopyridine (K_i = 90 μM), but is much less sensitive to TEA.

The differentiation inducer TPA causes dramatic alterations in this K^+ current. Upon addition of 10 nM TPA to the bath solution under whole-cell patch clamp conditions, current amplitude increases within 20 min, decreasing after this time (n=7). A decrease in current is similarly observed in the early stages of differentiation-induction in tissue culture (upon 4 h exposure to 0.5 nM TPA in 0.3% FBS) and this is accompanied by a much faster inactivation process (τ_i = 30 ms at 0 mV, n=5). The current becomes essentially undetectable in the later stages of differentiation (after 4 days). This K^+ current is present in KG1a cells, considered to represent a less mature differentiation stage than ML-1, but is absent from HL-60, which represent a slightly more mature differentiation stage. We conclude that a voltage-gated K^+ channel, regulated via PKC, may play a role in the early stages of the differentiation of hematopoietic myeloblasts.

M-AM-F6

SINGLE K CHANNELS RECORDED FROM MYELINATED AXON: THREE VOLTAGE-DEPENDENT, A CA-ACTIVATED, AN ATP-SENSITIVE, AND A FLICKERING BACKGROUND K CHANNEL

W. Vogel, P. Jonas*, M.E. Bräu, M. Hermsteiner, Duk-Su Koh, K. Kampe. Physiol. Inst., Aulweg 129, D-6300 Giessen, and *Max-Planck-Inst., Jahnstr. 29, D-6900 Heidelberg, FRG.

From the classical point of view vertebrate axons are equipped with only one type of potassium channel responsible for the termination of the action potential. Patch-clamp experiments on demyelinated fibers of *Xenopus* sciatic nerve (Jonas et al, Proc Natl Acad Sci 86:7238-42, 1989), however, allowed to identify not only one Na channel and three distinct potential-dependent K channels I, F and S which form the molecular basis of the former "delayed rectifier channel". We also detected three novel K channels which had so far not been observed in axonal membrane. The Maxi and the ATP-sensitive channel make novel links between metabolism and excitability now conceivable.

Channel type	γ [pS]	Density	Deactivation	Activation [mV]	Blocker TEA	Blocker other $K_{o.5}$ [mM]
I	23	+++	inter-mediate	-60..-30	+	Dendrotx, Charybdotx
F	30	++	fast	-40...60	+	
S	7	+	slow		+	
Maxi	132	++		Ca_i >-50	0.2	no Charybdotx
ATP-sens	44	++			4.2	0.035 ATP
Flicker	52	++		-	20	Cs, Zn, Ba

Single channel conductance (γ) measured at 15±2 °C in high external and internal K solution.

M-AM-F7

SURVIVAL OF K^+ CHANNELS IN SQUID NEURONS UPON DRUG BLOCK IN LOW EXTERNAL POTASSIUM.

F.T.Horrigan. Hopkins Marine Station of Stanford University, Pacific Grove, CA 93950.

Destabilization of K^+ channels in the absence of permeant cations has been previously demonstrated (Almers & Armstrong 1980, J.Gen.Physiol. 75: 61-78) The present investigation shows that K channel block, by open channel blockers, impairs survival of I_K in patch clamped squid giant fiber lobe neurons in the presence of low external and normal internal K^+. Methadone blocks voltage dependent I_K in a time dependent manner characteristic of open channel block. Recovery from block is slow and highly voltage dependent - consistent with drug "trapping" in a closed-blocked state. In normal external (10 mM) and internal (200-400 mM) K^+, the effects of methadone are completely reversible. However, in low external (0-2 mM) and normal internal K^+, methadone block induces a rapid and irreversible loss of activatible K^+ conductance. Currents evoked by 30 ms depolarizations (+40 mV) at 45 s intervals in 200 uM methadone (0 K^+,HP = -80mv) are kinetically identical, but decrease in amplitude with a time constant of 90 s. After drug washout, I_K kinetics and V-dependence appear identical to pre-drug controls but current amplitude remains reduced. The rate of I_K loss in 0 K^+-methadone is increased by increasing depolarization frequency, or by decreasing holding potential (slowing recovery from block). Open channel blockers other than methadone also induce I_K loss in low external K^+ (dibucaine, N-methyl-methadone) , but 4AP has no similar effect. I_K loss can be prevented but not reversed by 10 mM external K^+ or Cs^+; thus I_K loss does not simply reflect establishment of an abnormally long-lived blocked state in 0 K^+. These results also imply that a protective site in the channel pore remains accessible to external cations even during block. In conclusion, these experiments suggest the possibility that open channel blockers prevent access or binding of internal K^+ to a protective site while 4AP block or normal channel closing does not.

M-AM-F8

TWO PARADOXES FROM ONE CHANNEL. THE DELAYED RECTIFIER: ION PERMEATION AND BLOCKADE.

John R. Clay, NINDS, NIH, Bethesda, MD

An analysis of the effects of changes in the intra- and extracellular potassium ion concentrations on the instantaneous I-V relation of the delayed rectifier K^+ channel in internally perfused squid giant axons yields a paradox. Specifically, a change in K_o in the 0-500 mM range does not alter the outward current at strongly depolarized potentials (V > 60 mV), whereas the inward current is modified. Both results are consistent with Goldman-Hodgkin-Katz rectification, i.e., the independence principle (J.R. Clay & M.F. Shlesinger, Biophys. J. 42:43, 1983; J.R. Clay, Biophys. J. 45:481, 1984). Moreover, the slope conductance at 0 mV under equimolar conditions is a linear function of ion concentration for $K_i = K_o < 500$ mM. These results appear to be at odds with tracer flux ratio results, which suggest multiple occupancy of the channel by two or three ions (A.L. Hodgkin & R. D. Keynes, J. Physiol. 128:61, 1955; T. Begenisich & P. DeWeer, J. Gen. Physiol. 76:83, 1980). A second paradox concerns blockade of this channel by Cs^+. Blockade by Cs_o appears to occur at an electrical distance (from the external face of the channel) of ~0.9. Similarly, blockade by Cs_i appears to occur at an electrical distance (from the internal face of the channel) of 0.8-0.9. That is, a Cs ion from the inside seems to blithely pass over the blocking site for a Cs ion originating from the outside, and vice-versa. Is this not a paradox? Moreover, a Cs ion originating from the inside can pass through the channel, albeit sluggishly, at +200 to +250 mV under equimolar K^+ conditions, whereas a Cs ion originating from the outside has a very small probability of passing through the channel at -200 to -250 mV. Is this also not a paradox?

M-AM-F9

FIFTEEN SELECTIVITY SEQUENCES IN CHANNELS REVEALED BY A MICROSCOPIC MODEL. *Jin Wu, Department of Physiology, University of Rochester Medical Center, Rochester, NY 14642.*

A microscopic model is formulated by molecular kinetic theory based on Maxwellian and Boltzmann distributions to analyze selective ion permeation in channels. The selectivity filter used in the model consists of several axial symmetrically arranged carbonyl groups. Energy profiles, single channel conductances and the degree of hydration of K^+ in a hypothetical K^+ channel are evaluated by microscopic parameters: ion radius, ion mass, channel radius, number of effective water dipoles, number of site carbonyl groups etc. The i-V curve for K^+ in the channel is approximately linear up to ±170 mV. Channel radius and ion-water interactions are found to be two major channel structural determinants for selectivity sequences. Both ion radius and ion mass are important parameters in selectivity mediated by these interactions. The theory predicts a total of 15 possible conductance sequences (in symmetrical solutions) for alkali cations in ion channels with a single selectivity filter. Ten of these sequences are Eisenman sequences. However, IV_a, V_c, VI_a, VII, and $VIII_a$ are new.

I	*Cs>Rb>K>Na>Li*
II	*Rb>Cs>K>Na>Li*
III	*Rb>K>Cs>Na>Li*
IVa	*Rb>K>Na>Cs>Li*
V	*K>Rb>Na>Cs>Li*
VIa	*K>Rb>Na>Li>Cs*
VII	*K>Na>Rb>Li>Cs*
VIIIa	*K>Na>Li>Rb>Cs*
IX	*Na>K>Li>Rb>Cs*
X	*Na>Li>K>Rb>Cs*
XI	*Li>Na>K>Rb>Cs*
IVb	*K>Rb>Cs>Na>Li*
Vc	*Rb>K>Na>Li>Cs*
VIb	*K>Na>Rb>Cs>Li*
VIIIb	*Na>K>Rb>Li>Cs*

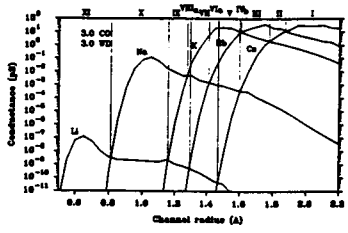

M-AM-G1

ANION PERMEABILITY OF GABA GATED CHANNELS IN ACUTELY ISOLATED PYRAMIDAL NEURONS FROM RAT HIPPOCAMPUS.

F.J. Alvarez-Leefmans*, M. Wakamori, T. Shirasaki, and N. Akaike. Department of Neurophysiology, Tohoku University School of Medicine, Sendai 980, Japan and *Departamento de Neurobiología, Instituto Mexicano de Psiquiatría, Calzada México-Xochimilco #101, México D.F., CP 14370, Mexico City.

The anion selectivity properties of GABA-gated channels in the membrane of acutely isolated CA1-pyramidal neurons from rat hippocampus were investigated using the whole-cell patch-clamp technique. Single neurons were isolated from 18 day-old Wistar rats following an enzymatic cell dissociation method similar to that of Kaneda et al (Neurosci. Res., 5, 299-315, 1988). Whole-cell currents were induced by pressure application of GABA (3×10^{-6} M) in the vicinity of the neuronal cell body, by using the "Y-tube method" (Akaike et al, Acta Physiol. Scand. 136, Suppl. 582, 21, 1989). This allowed the exchange of the external solution surrounding the cell within 20 msec. The same device was used to produce rapid changes in the anion composition of the fluid surrounding the cell. The pipette solution contained (in mM): 130 CsCl, 17 NaCl, 0.5 $CaCl_2$, 1 $MgCl_2$, 5 EGTA, 2 ATP-Mg,10 HEPES, pH 7.2. The standard external solution (SES) contained (in mM): 139 NaCl, 5 CsCl, 2.5 $CaCl_2$, 1 $MgCl_2$, 10 glucose, 10 HEPES, pH 7.4. The permeability of the channels to other anions (A^-) relative to Cl^- was determined by replacing 100 mM NaCl from the SES with the Na-salt of each of the anions tested. The Cl^- activity of all the solutions was measured with a Chloride Selectrode (Radiometer). The reversal potential of GABA-induced whole-cell currents (E_{GABA}) measured in SES had the same value as the Cl^- equilibrium potential (E_{Cl}). The following permeability ratios, P_{A^-}/P_{Cl^-}, were calculated from the Goldman-Hodgkin-Katz potential equation: SCN^- 6.69, I^- 2.41, NO_3^- 2.01, Br^- 1.54, ClO_3^- 1.2, Formate 0.82, Acetate 0.16, HCO_3^- 0.15, BrO_3^- 0.15, Propionate 0.13, Fluoride 0.04.

M-AM-G2

Voltage-dependence of GABA desensitization in chick cerebral neurons. John J. Hablitz, Neurobiology Research Center, University of Alabama at Birmingham, Birmingham, Alabama 35294

The whole cell patch clamp recording technique was used to study GABA desensitization in chick cerebral neurons. GABA (10-100 μM) was applied by rapid perfusion, and measurements were made of GABA-gated chloride currents and associated conductance increases. GABA currents declined during prolonged (5-10 s) agonist applications. This was associated with a decline in the conductance increase induced by GABA, suggesting it was due to receptor desensitization. By examining GABA responses at different holding potentials it was found that desensitization was voltage dependent. At a holding potential of -60 mV, the conductance increase in response to 100 μM GABA declined by over 50%, whereas at 0 mV, it declined by approximately 30%. Desensitization was not observed when GABA was applied at holding potentials of +40 - +60 mV. In most neurons, the decrease in conductance followed a single exponential time course with a decay time of 6-9 s at -60 mV. A second faster exponential component was present in some cells but was not characterized. Decay times of 15-20 s were observed at 0 mV. Similar results were obtained with 10 μM GABA although desensitization was slower. The chloride equilibrium potential was varied from -70 to 0 mV by using, in different cells, different intracellular chloride concentrations. A similar voltage dependence of desensitization was observed, suggesting that it is voltage, not chloride movement, that is affecting the rate of desensitization. These changes in desensitization could result in enhanced GABAergic transmission upon depolarization. Supported by NS 18145.

M-AM-G3

GLUTAMATE-INDUCED LONG-TERM POTENTIATION OF MINIATURE EPSP FREQUENCY IN CULTURED HIPPOCAMPAL NEURONS. A. Malgaroli & R. W. Tsien, Department of Molecular and Cellular Physiology, Stanford CA 94305.

There is great interest in possible presynaptic and postsynaptic contributions to the expression of long-term potentiation (LTP). Analysis of miniature epsps, a classical approach to synaptic phenomena, is difficult in brain slice LTP because it is unclear whether individual minis arise from potentiated or unpotentiated synapses. To circumvent this problem, we recorded from hippocampal pyramidal cells in culture and used direct and global application of glutamate to induce synaptic enhancement. Dissociated hippocampal pyramidal neurons were obtained from 2-3 day-old rat pups and kept in culture for 7-10 days before use. Large neurons with CA1-like morphology were studied with whole-cell recordings with pipettes containing (mM) 110 Cs-gluconate, 10 NaCl, 5 $MgCl_2$, 2 ATP, 0.2 GTP, 0.6 EGTA, HEPES (pH 7.2 with CsOH). The neurons form synapses in culture as detected by evoked and spontaneous synaptic currents and synapsin I immunostaining. We found that mini frequency was strongly increased in 18/23 cells by a 30 s exposure to 25-50 μM glutamate; a typical increase was ~3-fold. The enhancement was seen despite the presence of 1 μM TTX to block electrical activity. Like LTP, the enhancement of mini frequency was (1) persistent up to the end of the recording (as long as ~80 min); (2) mediated by NMDA receptors, as judged by reversible block with the NMDA receptor channel blocker MK801 (10 μM); (3) specific for excitatory but not inhibitory minis (1 cell). In almost all cases, the distribution of mini amplitudes was not significantly changed before and after glutamate application. Postsynaptic responsiveness was also tested directly with brief puffer applications of glutamate, and remained unchanged during the enhancement of mini frequency. This excludes the possibility that mini frequency increased because of recruitment of previously latent spines. Our results indicate that enhancement of presynaptic transmitter release can be achieved by glutamate receptor activation even in the presumed absence of presynaptic action potentials. Thus, the synaptic enhancement might result from increased efficiency of other steps in neurosecretion, such as those controlling vesicle availability or vesicle fusion and exocytosis.

M-AM-G4

LONG-TERM POTENTIATION OF HIPPOCAMPAL SYNAPTIC TRANSMISSION AT RAPID STIMULUS RATES. F.E. Schweizer, J.A. Kauer, R.W. Tsien, Department of Molecular and Cellular Physiology, Stanford Medical Center, Stanford CA 94305

Quantal analysis is a promising approach for studying the mechanisms of synaptic plasticity in the hippocampus. We have tried to find conditions that aid quantal analysis of synaptic changes during long-term potentiation (LTP). Minimal stimulation of the Schaffer collateral pathway evokes epscs which can be recorded from CA1 pyramidal neurons in rat hippocampal slices. The whole cell voltage clamp recording method provides superior signal-to-noise characteristics but limits the period during which LTP can be consistently induced (Malinow & Tsien, 1990). Raising the frequency of synaptic stimulation from 0.25 Hz to 2 Hz may allow the acquisition of sufficient numbers of epscs for quantal analysis, and also minimizes the impact of slow changes in synaptic properties. However, previous studies using microelectrode recordings have encountered difficulties in inducing LTP at rapid stimulation rates.

We have looked for LTP at increased stimulus rates in whole cell recordings. Rapid stimulation (1.67-2 Hz) did not produce potentiation by itself. During the control period, before attempting to induce LTP, the synaptic strength often declined gradually. The magnitude of depression was quite variable, but generally did not exceed 50% (values ranged from zero to almost 100%). The depression was accompanied by an increased number of failures; decreased Ca^{2+} delivery may have been a factor, since the introduction of a second stimulus 30-40 msec after the first was effective in producing a synaptic response.

We were able to observe significant potentiation in about half of the experiments (19 of 31 cells). The potentiation was accompanied by an immediate decrease in the proportion of synaptic failures (mean decrease of 45%, range 10-86%). This observation supports the notion that potentiation is expressed presynaptically. The amplitude of the potentiated epscs sometimes declined over the first 20 minutes, but the mean epsc usually remained potentiated for the duration of the recording. The magnitude of the synaptic enhancement was not apparently correlated with the amount of depression during the control period. The finding that potentiation can be induced under conditions of rapid stimulation augurs well for a rigorous analysis of quantal properties before and after LTP.

M-AM-G5

ELECTROPHYSIOLOGICAL AND IMMUNOCYTOCHEMICAL CHARACTERIZATION OF CULTURED SUBSTANTIA NIGRA NEURONS IN RELATION TO DOPAMINE RECEPTOR SUBTYPES.

K-M. Kim, Y. Nakajima and S. Nakajima, Dept. of Pharmacology and Dept. of Anatomy and Cell Biology, Univ. of Illinois College of Medicine, Chicago, IL 60612.

We separately cultured from the pars compacta and the pars reticulata of the substantia nigra using 2 to 4-day old postnatal rats. Using antibodies to tyrosine hydroxylase (TH) and GABA, we have immunocytochemically identified four kinds of neurons in these cultures: (1) Dopaminergic (DA) neurons, TH(+) GABA(-); (2) GABA neurons, TH(-) GABA(+); (3) Non DA-non GABA neurons, TH(-) GABA(-); and (4) DA-GABA neurons (very rare, TH(+) GABA(+)).

Using the whole cell clamp method, we have conducted D_2 receptor studies mainly on 15-21 day cultured neurons from the pars compacta and D_1 receptor studies mainly on 4 to 8 week cultured neurons from the pars reticulata. When the cell was clamped at -74 mV, D_2 agonists (dopamine, (-)-quinpirole) increased the membrane conductance concomitant with an outward current, indicating an increase in K-conductance. In contrast, D_1 agonists (dopamine, R(+)-SKF38393) generally decreased the membrane conductance concomitant with an inward current. Following electrophysiological experiments neurons were immunocytochemically treated. Cells in which D_2 agonists elicited an increase in K-conductance were dopaminergic (TH(+) GABA(-)). In contrast, cells which responded to D_1 agonists were non DA-non GABA (TH(-) GABA(-)). Supported by PHS grants, DA05701 and NS24711.

M-AM-G6

POLYAMINES POTENTIATE NMDA RESPONSES OF RECEPTORS EXPRESSED IN *XENOPUS* OOCYTES. J.F. McGurk, R.S. Zukin and M.V.L. Bennett. Albert Einstein Col. Med., Bronx, NY 10461.

Glutamate, the major excitatory neurotransmitter in the central nervous system, activates at least three types of channel-forming receptors defined by the selective agonists N-methyl-D-aspartate (NMDA), kainate and quisqualate (or AMPA). Activation of the NMDA receptor requires glycine as well as NMDA, glutamate or other agonist. Recent studies have shown that certain polyamines potentiate binding by NMDA receptors of glycine and the open channel blocker MK-801. To determine whether polyamines alter channel opening, we examined their effects on rat brain glutamate receptors expressed in *Xenopus* oocytes. Spermine potentiated NMDA responses but had no effect on responses to kainate and quisqualate. Conductances were increased up to threefold with no change in reversal potential. Onset and recovery were rapid (<0.5 s, limited by application time), indicating action extracellulary rather than through uptake or a second messenger. Spermine alone had no effect. Spermidine also potentiated NMDA responses; putrescine did not. Instead, putrescine reduced spermine potentiation, possibly competitively. Spermine potentiation increased with concentration (apparent K_d ~40 μM, Hill coefficient ~ 2.0) and then declined above 250 μM, perhaps due to autoinhibition. Spermine produced a leftward shift in the concentration response curve for glycine, reducing the K_d (from ~ 930 to ~ 330 nM). Thus, the degree of potentiation depended on the glycine concentration. At saturating levels of glycine (10 μM), 250 μM spermine increased the peak response approximately 2-fold versus control. At 0.1 μM glycine, 250 μM spermine increased the peak response about 3-fold. The K_d and Hill coefficient for NMDA were not affected by spermine, and the degree of potentiation did not depend on NMDA concentration. The Hill coefficient and K_d for spermine were not affected by glycine or NMDA concentration. Spermine acts, at least in part, by increasing the apparent affinity for glycine. Spermine may have an additional action, since the response at saturating glycine is increased. Polyamines are a natural constituent of brain in pharmacologically significant amounts in the tissue as a whole, but concentrations in interstitial fluid are unknown. Polyamines may prove to play a role in modulation of glutamatergic transmission at NMDA receptors.

M-AM-G7

PRESYNAPTIC QUANTAL RELEASE IS SPECIFIED BY POSTSYNAPTIC NEURONS IN BUCCAL GANGLIA OF *APLYSIA*.

Daniel Gardner, Dept. of Physiology and Biophysics, Cornell University Medical College, New York, NY 10021.

In the buccal ganglia of *Aplysia*, cells B4 and B5 mediate parallel actions upon their population of follower cells; in particular, they produce similar inhibitory PSCs in several postsynaptic neurons. The synaptic strengths of these connections vary, due to synapse-to-synapse differences in amplitude and duration of the underlying synaptic conductances, with long-term synaptic strengths specified by the postsynaptic neuron. PSC amplitudes are thus similar for inputs from B4 and B5 converging on a postsynaptic cell, but different for branches of the same neuron diverging onto different targets. I now report that these differences in synaptic amplitude reflect differences in quanta released by presynaptic terminals of B4 and B5, rather than a postsynaptic factor such as receptor sensitivity.

Recording from B4, B5, and two voltage-clamped postsynaptic cells allows analysis of four similar synapses sharing common presynaptic and postsynaptic cells in the same preparation. Peak conductance (g_{peak}) was determined for sets of PSCs at each of 50 synapses for which g_{peak} was stationary. For each synapse, mean and variance of g_{peak} were used to derive quantal parameters consistent with a simple binomial model and assuming that fluctuations in amplitudes of sequential PSCs represent differences in quantal release, rather than receptor number, desensitization, or noise. PSC ensemble variance time course was consistent with this view. The indirect analysis permits factoring g_{peak} into $m/(1-p)$ [upper limit of estimated quantal content, and a purely presynaptic factor] and $\gamma(1-p)$ [lower limit of quantal conductance change, largely postsynaptic].

Both g_{peak} and estimated quantal content $m/(1-p)$ varied over almost two orders of magnitude, with $m/(1-p)$ ranging from 17 to 2770. For these data, $\log_e [m/(1-p)]$ was correlated with $\log_e [g_{peak}]$ (r=0.87, slope = 1.1), consistent with differences in quantal release underlying different mean synaptic strengths. In contrast, $\gamma(1-p)$ [1.14 ± 0.11 nS] showed less variation and was independent of g_{peak} (r=0.19).

Pairing quantal values by common pre- or postsynaptic cells shows that $m/(1-p)$ is similar for presynaptic endings converging on a single follower (P=0.0001) but different for endings of the same presynaptic cell on different targets (P=0.34); log ratio indices confirm the ANOVA. No pairing specificity is seen for $\gamma(1-p)$.

Varying postsynaptic specification of release from presynaptic terminals may involve dynamic retrograde modulation, as in hippocampus.

M-AM-G8

CONDUCTANCE PROPERTIES OF GLYCINE-ACTIVATED CHLORIDE CHANNELS DEPEND ON CYTOPLASMIC CHLORIDE CONCENTRATION. A. I. McNiven, R. L. DeGrandchamp and A. R. Martin. Department of Physiology, Univ. of Colorado School of Medicine, Denver CO 80262.

Neurons from mouse spinal cord were maintained in culture for 2 - 4 weeks. Antibody staining indicated the presence of glycine receptors on the soma and basal processes of individual cells. Presentation of 10 µm glycine to the outer face of outside-out membrane patches activated chloride channels with main conductance states of about 19 pS ($[Cl]_{electrode}$ 7 mM, $[Cl]_{bath}$ 157 mM). The variance of the open channel amplitude distribution was usually similar to the baseline variance, as openings to lower conductance substates were few. When $[Cl]_{electrode}$ was 20 mM, the channel conductance increased to about 25 pS. However, with the higher cytoplasmic chloride concentration, the open channel amplitude distributions were markedly skewed to the left, because of increased numbers of openings to lower conductance substates. The effect of the increased substate openings was to decrease the average channel conductance. Thus increasing chloride concentration on the cytoplasmic face of the patch not only increased channel conductance but also altered the distribution of channel open states. We conclude that this mechanism is responsible for the decrease in mean channel conductance with increased intracellular chloride concentration observed previously with noise analysis of glycine-activated channels in reticulo-spinal neurons (Gold, M. R. and Martin, A. R. J. Physiol. 349: 99, 1983).

Supported by Grant #NS09660 from the National Institutes of Health.

M-AM-H1

^{19}F NMR STUDIES OF BACTERIAL CHEMOSENSORY PROTEINS.

Joseph J. Falke and Linda A. Luck.

Department of Chemistry and Biochemistry, University of Colorado 80309-0215.

Conformational changes play an important role in sensory and signaling proteins. These changes regulate the interaction between an activated protein and its target protein or nucleic acid. We have found that solution ^{19}F NMR can reveal key features of conformational changes even in proteins too large for NMR structure determination. Here we describe ^{19}F NMR studies of two chemosensory proteins of the E.coli chemotaxis system: the periplasmic D-galactose and D-glucose receptor (GGR), and the cytoplasmic "switch" protein (CheY) which regulates the rotational sense of the flagellar motor.

The crystal structure of GGR is known and reveals a sugar binding cleft between two distinct domains, as well as a surface Ca(II) binding site closely related in structure to the eukaryotic EF-hand sites (F. A. Quiocho et al.). Activation of this receptor by sugar binding induces changes in surface structure which enable it to dock to membrane transducer and transport proteins. Our ^{19}F NMR studies, which have incorporated fluorinated trp and phe residues into GGR, indicate that sugar binding induces a conformational change detected at 11 of 12 sites distributed throughout the protein. This global structural change involves spatial shifts of multiple alpha helices and beta strand elements. In contrast Ca(II) binding induces a localized conformational change in which only 3 of the 12 sites exhibit ^{19}F NMR frequency shifts.

The model for the sugar-induced conformational change in GGR suggests that the empty cleft exists in an open conformation, but the structure of the empty cleft is unknown. We have compared the structures of the D-glucose occupied and empty clefts by ^{19}F NMR using an aqueous paramagnetic broadening agent. The results reveal that the empty cleft opens at least transiently by an angle of 15^{o} in solution.

^{19}F NMR studies comparing the phosphorylated (D13K) and dephosphorylated conformations of CheY will also be discussed.

M-AM-H2

TACTIC RESPONSES OF BACTERIA TO CAGED PHOTORELEASE OF PROTONS

Shahid Khan, Kwame Amoyaw, John L. Spudich.

Departments of Anatomy & Structural Biology and Physiology & Biophysics. Albert Einstein College of Medicine, Bronx, N.Y 10461.

A time resolved behavioral assay for measurement of tactic responses of free swimming populations of bacteria has been developed. The assay depends on coupling flash photorelease of caged compounds (McCray and Trentham. 1989. Ann Rev. Biophys. Biophys. Chem. 18,239-270) to computer assisted motion analysis (Sundberg et al. 1986. Biophys. J. 50,895-900). Measurements of response times of bacteria upon caged photorelease of protons will be presented. Response times shorter than 100 milliseconds have been measured using the assay. Bacteria with sodium powered as well as proton powered motile systems respond to pH shifts. This implies that the pH sensor does not require a motor driven by protonmotive force. In *Escherichia coli*, the nature and kinetics of the response to pH decreases depend upon the initial pH. These measurements complement and extend published biochemical studies of pH responses in this bacterium (Repaske and Adler. 1981. J. Bacteriol, 145,1196-1208: Kihara and Macnab. 1981. J. Bacteriol. 145,1209-1221: Slonczewski et al. 1982. J. Bacteriol. 152,384-399).

M-AM-H3

SIGNAL TRANSDUCTION IN *PHYCOMYCES* PHOTOTROPISM.

E. Lipson[1], X. Chen[1], P. Schmidt[1], B. Horwitz[2], D. Baum[2], D. Rosenblatt[2], T. Short[3] and W. Briggs[3]. [1]Department of Physics, Syracuse University, Syracuse, NY, 13244; [2]Department of Biology, Technion, Haifa 32000, Israel; and [3]Department of Plant Biology, Carnegie Institution of Washington, Stanford, CA 94305.

The Zygomycete fungus *Phycomyces* responds to blue light stimuli over the intensity range from 10^{-9} to 10 W·m^{-2}. The responses of the aerial sporangiophore include phototropism and the related light-growth response. A collection of well characterized behavioral mutants includes some with defects in the photoreceptor system. To investigate the molecular basis of *Phycomyces* light responses, we are examining pathways generally implicated in signal transduction processes. In behavioral assays with sporangiophores immersed in solutions, the following chemicals were tested for their effects on growth rate and phototropism. Millimolar concentrations of calcium reduced both growth and phototropism. The calcium ionophore A23187 (> 10 μM) reduced growth slightly and strongly suppressed phototropism. Addition of EGTA (up to 5 mM) did not affect growth or phototropism (perhaps because the chelator was not taken up by the sporangiophore), except for a possible growth enhancement in the 1-100 μM range. Cyclic AMP (> 100 μM) inhibited phototropism, but the growth rate remained normal. The auxin indoleacetic acid (> 0.1 mM) reduced growth and phototropism. These results suggest that calcium, cAMP, and indoleacetic acid may participate in photosensory transduction or at least in growth regulation in *Phycomyces*. Measurements of inositol lipid and inositol trisphosphate levels following light stimulation are in progress. On a Western blot with an antibody against a synthetic peptide corresponding to the conserved carboxyl terminus of the transducin α subunit, a ~50 kDa protein was revealed consistently in extracts of sporangiophores from wild type and various mutant strains; this may represent a G protein that could play a role in the responses. Finally, in preliminary studies, we have found that *in vivo* illumination enhances *in vitro* phosphorylation of a 40 kDa microsomal protein. In some mutants, the phosphorylation appears weaker than in the wild type strain. A Western blot indicates that the 40 kDa protein cross reacts with a 120 kDa phosphorylated protein implicated in plant phototropism. (Supported by grant GM29707 from the National Institutes of Health and grant 86-00302 from the U.S.-Israel Binational Science Foundation)

M-AM-H4

THEORETICAL STUDIES ON FLAGELLAR MOTOR ROTATION BASED ON THE CROSS BRIDGE FORMALISM

Yi-der Chen[1] and Shahid Khan[2]
1. LCP, NIH, Bethesda, MD 20892.
2. Dept. Anatomy & Structural Biology and Dept. Physiology & Biophysics, Albert Einstein College of Medicine, Bronx, NY 10461.

The general procedure is described for the calculation of angular rotation velocity of a flagellar motor based on the muscle contraction formalism of Hill[1]. We assume that each stator can exist in two (or more) conformations and undergo cyclic biochemical reactions involving binding of protons (or other ions, such as sodium) and attachment to the sites on the rotor. In one conformation, a stator is accessible only to the protons on the outside of the membrane and in another conformation to those on the inside[2]. The mode of attachment of a stator to a rotor site is conformation-dependent. Torque is generated only when a stator is attached to a rotor site. Both the differential equation method and the Monte Carlo simulation are described and applied in a relatively simple case. Comparisons with other theoretical treatments are discussed.

(1). Hill, T. L., Prog. Biophys. Mol. Biol. 28, 267-340 (1974).
(2). Khan, S., Dapice, M. and Humayun, I., Biophys. J. 57, 779-796 (1990).

M-AM-H5

MOTOR RESPONSES OF HALOBACTERIUM HALOBIUM TO GRADED LIGHT STIMULI.

S. Lucia, C. Ascoli, D. Petracchi (Intro. by E.N. Spudich)
Istituto di Biofisica CNR, Via S. Lorenzo 26, 56127 Pisa,Italy.

Sinusoidal and saw-tooth light stimuli have been used to elicit photoresponses in Halobacterium halobium strain Flx 15. Both the mean level of the light and its modulation depth have been varied independently. Interval histograms, cycle histograms and autocorrelation functions have been used in the data analysis. Cycle histogram and autocorrelation function evidentiate the stimulus periodicity even for low modulation depth and very slow stimuli, up to a period of 80 sec. A lower limit for the light gradient which can be detected by Halobacterium halobium is extrapolated. Responses at different light level and different modulation depth have been obtained. The results show that a very effective parameter of the stimulus is the modulation depth, whereas the responses are only slightly affected by the mean light level.

M-AM-H6

THE EFFECTS OF GROWTH IN HIGH IONIC STRENGTH MEDIA ON MOTILITY AND CHEMOTAXIS OF ESCHERICHIA COLI

C. Li[3], C. Louise[1] & J. Adler[1, 2] (Intro. by Y. Saimi)
Departments of Biochemistry[1] & Genetics[2], Program in Cellular & Molecular Biology[3], University of Wisconsin-Madison, Madison, Wisconsin 53706

The bacterium E. coli migrates towards favorable environments and away from unfavorable environments. E. coli derives its motility from the use of flagella. The genes involved in flagellation and motility are organized into a regulon. Expression of this regulon is positively regulated by cAMP, and affected by many environmental stimuli.

We found that motility was repressed when E. coli was grown in media containing high salts. Motility was assayed by two methods. The first method used was to observe cells microscopically while videotaping them. The videotapes were subsequently analyzed by computer. The second method involved using a swarm plate assay. Bacteria were placed in semi-solid agar medium in which motile bacteria form a swarm pattern while nonmotile bacteria do not. The number and length of flagella produced in high and low salt media were determined by flagellar staining. Cells grown in low salt media produced both longer and a greater number of flagella. Flagella were sheared from cells grown in low or high salt media and flagellar protein was detected by SDS gel electrophoresis. No flagellin protein was observed in cells grown in high salt media. Motility of mutants not requiring cAMP for flagellar synthesis was repressed by growth in high salt media. This indicated that the effect of growth in high salt was not due to catabolite repression. We hypothesize that the effect of growth in high salt media is partially due to the high osmolarity of the media. Mutants which are motile in high salt media were isolated and characterized. The behavioral and genetic analyses of these mutants are in progress.

M-AM-I1

BLOCKING OF THE CA^{2+}-INDUCED OPENING OF INTERHELICAL INTERFACES IN EITHER OF THE TWO DOMAINS OF CALMODULIN RENDERS THE PROTEIN INACTIVE. Z. Grabarek, R.-Y. Tan and J. Gergely, Department of Muscle Research, Boston Biomedical Research Institute, Boston MA 02114

Restriction of the Ca^{2+}-induced movement of pairs of α-helical segments in the N-terminal or in the C-terminal domain of troponin C leads to a loss of the Ca^{2+}-sensitizing activity or a dramatic decrease in affinity for troponin I, respectively (Grabarek et al. Nature 345, 132, 1990; Grabarek et al. this Meeting. To see whether similar transitions are required for the Ca^{2+}-induced activation by calmodulin (CaM) of its target enzymes, Cys residues were introduced by site directed mutagenesis into corresponding locations replacing Q41 and K75 in the N-terminal domain (CaM41/75) or I85 and L112 in the C-terminal domain (CaM85/112),(cDNA of human liver CaM kindly provided by Dr. R. N. Perham, Cambridge, UK). In both mutants stable disulfide bonds were readily formed as evidenced by the effect of DTT on electrophoretic mobility on native gels. The disulfide containing mutants further purified on reverse phase HPLC were unable to activate phosphodiesterase or calcineurine even at μM concentrations. The lack of activity results from the failure to bind to the target enzymes since no competitive inhibition of the wild type CaM by the mutant could be detected. Upon reduction of the disulfide with DTT and blocking the Cys residues with iodoacetamide CaM41/75 did recover full activity with respect to both enzymes. Only partial activity could be recovered in the case of CaM85/112. The changes in Kd and Vmax could be substantially reversed by blocking of Cys with less polar CN groups suggesting that the hydrophobic side chains of Ile85 and Leu112 may be involved in CaM's interaction with target enzymes. Our results indicate that the Ca^{2+}-induced opening of the interhelical interfaces in both domains are necessary for binding and activation of target enzymes by CaM. Supported by NIH, AHA, MDA.

M-AM-I2

LIGAND-LINKED CONFORMATIONS OF CALMODULIN

Susan Pedigo, Amy S. Verhoeven, Wolfgang A. Schaller & Madeline A. Shea
Dept. of Biochemistry, U. of Iowa College of Medicine, Iowa City, IA 52242

Cooperative binding of divalent cations to calmodulin causes large conformational changes that permit it to activate a wide range of target enzymes. The position as well as number of ions bound may control activation. In an effort to determine which of many possible macromolecular species are functionally significant, we are monitoring individual sites and individual species of calmodulin to identify and quantitate the populated intermediate states.

We have probed ligand-linked conformational changes of calmodulin by investigating changes in proteolytic susceptibility. Chemical reagents and both specific and non-specific proteases were applied under conditions of limited proteolysis. Products were screened electrophoretically and quantitated using reversed phase HPLC; amino acid analysis was used to identify the resulting peptide fragments. From these data we determined primitive isotherms or reactivity profiles and found that divalent ion binding to calmodulin protected it from cleavage at most positions; however, there were notable exceptions. Fragments manifested a wide range of electrophoretic mobility shifts as a function of ligand levels, pH and buffer composition. Conformations of peptides containing the third site were most sensitive to saturation; peptide composition beyond the site also strongly influenced folding properties. We have trapped and separated distinct ligation species on the basis of differential cryogenic (-50 C) electrophoretic transport properties.

[Supported by N.S.F. P.Y.I. award to M. A. Shea.]

M-AM-I3

PHOSPHORYLATION DEPENDENT BINDING OF A SYNTHETIC MARCKS PEPTIDE TO CALMODULIN. Brian K. McIlroy, John D. Walters, Perry J. Blackshear, and J. David Johnson The Ohio State University and Duke University

The MARCKS protein is a major substrate for protein kinase C (PKC). A highly conserved 25 amino acid sequence (KKKKKRFSFKKSFKLSGFSFKKNKK), containing the four PKC phosphorylation sites and the calmodulin (CaM) binding domain, was used to determine the effects of phosphorylation on its binding and regulation of CaM.

PKC phosphorylation of this peptide (3.0 mole P_i/mole peptide) produced a 200-fold decrease in its affinity for CaM and prevented the peptide from inhibiting CaM's activation of phosphodiesterase (PDE). PKC phosphorylation of the peptide resulted in its dissociation from CaM over a time course which paralleled the phosphorylation of 1 mole ser/mole peptide. The peptide inhibited CaM's binding to myosin light chain kinase (MLCK) and CaM's stimulation of PDE and calcineurin. PKC phosphorylation of the peptide resulted in a rapid release of bound CaM, allowing its subsequent binding to MLCK ($t_{1/2}$= 1.6 min.), stimulation of PDE ($t_{1/2}$= 1.2 min.) and stimulation of calcineurin ($t_{1/2}$= 1.7 min.). The partially purified MARCKS protein produced a similar inhibition of CaM-PDE that could be reversed by PKC phosphorylation. The primary sites of PKC phosphorylation of the peptide were at ser 8 and ser 12. Peptide affinity for CaM was primarily controlled by phosphorylation of ser 12.

Our results demonstrate that PKC phosphorylation of the peptide and the MARCKS protein results in the rapid release of CaM and the subsequent activation of CaM-dependent enzymes. This process might allow for interplay between PKC-dependent and CaM-dependent signal transduction pathways within the cell.

M-AM-I4

EFFECTS OF CA^{2+}/CAM KINASE II INHIBITOR (KN-62) ON REGULATORY MECHANISMS OF CYTOSKELETAL ELEMENTS.

Hiroyoshi Hidaka, Hiroshi Tokumitsu, Akihiro Mizutani, and Motomu Terasawa.
Department of Pharmacology, Nagoya University School of Medicine, Showa-ku, Nagoya 466, Japan.

Calmodulin is now widely accepted as a major intracellular receptor for calcium ion. A central role of calmodulin is thought to be regulation of the activity of many enzyme in a Ca^{2+}-dependent manner, and interaction with cytoskeletal proteins. We have recently found a Ca^{2+}/calmodulin-dependent protein kinase activity and its endogenous substrate (vimentin) in cytoskeletal fraction of rat embryo fibroblast 3Y1 cells. This enzyme was tightly associated to cytoskeletal elements, and showed the same properties as brain Ca^{2+}/CaM kinase II. Furthermore, this endogenous phosphorylation induced by calmodulin was inhibited by addition of a Ca^{2+}/CaM kinase II specific inhibitor (KN-62), in a dose dependent manner. These results suggested that cytoskeleton associated calmodulin dependent protein phosphorylation was not specific for neuronal tissue as post synaptic density, and was an important propose for the regulation of the cytoplasmic space through Ca^{2+}/calmodulin pathway.

KN-62 is a potent and selective inhibitor to Ca^{2+}/CaM kinase II activity, which include both exogenous substrate phosphorylation and autophosphorylation. Kinetical analysis showed that KN-62 inhibited the activity of Ca^{2+}/CaM kinase II competitively with respect to calmodulin. In addition, KN-62 inhibited the Ca-ionophore induced autophosphorylation of Ca^{2+}/CaM kinase II in PC12D cells, suggesting that the inhibitor had a cell membrane permeability and blocked the Ca^{2+}/CaM kinase II activity in intact cells. In further study, to elucidate the physiological role of Ca^{2+}/CaM kinase II, we tried to examine the effects of KN-62 on the phosphorylation of a novel calmodulin binding protein from bovine brain (ACAMP-81) and of phospholamban (PL), in cardiac SR membrane. Phosphorylation of ACAMP-81 and PL by Ca^{2+}/CaM kinase II was also inhibited by KN-62 *in vitro*. These findings suggest that KN-62 is a useful pharmacological probe for studying the physiological significance of Ca^{2+}/CaM kinase II in intact cells and tissues.

M-AM-15

CA^{2+} BINDING SITES: MOLECULAR MECHANISMS OF SUBSTRATE SPECIFICITY.

Joseph J. Falke, Brian W. Buoscio, Eric E. Snyder, Kay C. Thatcher, and C. Stefan Voertler.

Department of Chemistry and Biochemistry, University of Colorado, Boulder, Colorado 80309-0215

Protein Ca^{2+} binding sites selectively bind Ca^{2+} while excluding much higher (up to 10^5-fold) concentrations of Na^+, K^+, and often Mg^{2+}. This specificity is particularly important for regulatory sites which must remain empty until a Ca^{2+} burst, and for Ca^{2+} channel sites which block transmembrane leaks of certain other cations. The Ca^{2+} binding site of the E. coli D-galactose and D-glucose receptor has been shown to be useful as a model site because its substrate specificity can be easily quantitated while its structure is similar to the EF-hand class of Ca^{2+} sites found in eukaryotic Ca^{2+}-regulated proteins. Like other sites the bacterial site uses a pentagonal bipyramidal array of seven oxygens to coordinate bound metal ion. Here we report an investigation of the molecular mechanisms by which this oxygen array discriminates potential substrates on the basis of ionic radius and charge.

We have engineered changes in the cavity size and negative charge density of the coordinating array by replacing glutamine 142 with asparagine, glutamate, and aspartate. The substrate specificity of each engineered site has been quantitated using a Tb^{3+} fluorescence assay to determine the binding free energies for a series of spherical metal ions of different size and charge: the Group Ia, IIa, IIIa and lanthanide metal ions. Sites containing an engineered smaller sidechain (asn or asp) exhibit altered size specificities, yielding up to 50-fold higher affinities for large cations than the native site. And sites containing an engineered acidic sidechain (glu or asp) exhibit altered charge specificities, yielding selectivities for trivalent over divalent ions 300-fold higher than the native site. The results verify that the cavity size and negative charge density of the coordination array play key roles in the control of substrate specificity, and that Ca^{2+} binding sites can be engineered to specifically bind other metal ions.

M-AM-16

IDENTIFICATION OF CALCIUM BINDING DOMAINS IN CALRETICULIN

S. Baksh, K. Burns and M. Michalak.
Departments of Biochemistry and Pediatrics, University of Alberta, Edmonton, Canada T6G 2S2

Calreticulin is one of several Ca binding proteins found in sarcoplasmic reticulum (SR) and endoplasmic reticulum (ER) membranes. It is localized within the lumen of the SR/ER and it is thought to contain both high-capacity low-affinity, and low-capacity high-affinity binding sites for Ca. We have isolated a cDNA clone encoding calreticulin from rabbit skeletal muscle, and have deduced the amino acid sequence of the protein from the nucleotide sequence of this cDNA (Fliegel, *et al.* (1989) J. Biol. Chem 264:21522-21528).

Here we propose a folding model for calreticulin based on the deduced amino acid sequence, and describe studies which aim to determine the Ca binding site(s) in the protein. The protein sequence (401 amino acids in length) begins with a helix-turn-helix motif, which is followed by 8 anti-parallel ß-strands connected by protein loops (*ß-strands domain;* N-terminal half of the protein). This is followed by a sequence containing an abundance of prolines, some of which are spaced regularly every 4 or 5 amino acids (*P-rich domain;*~100 amino acids in length). The C-terminal 20% of the protein is highly acidic (*acidic tail domain;*~100 amino acids in length). Calreticulin terminates with the KDEL ER retention sequence. We have subcloned and expressed, as a glutathione S-transferase fusion protein, the C-terminal *acidic tail* and *P-rich* domains. The glutathione S-transferase-calreticulin fusion proteins were isolated and assayed for Ca binding. Our results indicate that both domains are involved in Ca binding to calreticulin.

(Supported by MRC, AHSF and AHFMR)

M-AM-J1

GENE AMPLIFICATION OF VOLTAGE-GATED SODIUM CHANNELS FROM HUMAN BRAIN, HEART, AND SKELETAL MUSCLE. J.H. Caldwell and K.L. Schaller, Department of Cellular and Structural Biology, University of Colorado Health Sciences Center, Denver, Colorado 80262

The polymerase chain reaction (PCR) has been used to isolate Na channel genes from a variety of human tissues. Oligonucleotide primers were chosen to amplify the cDNA between IIIS3 and IVS1. The length of the amplified DNA should be about 850 nucleotides. RNA was isolated and reverse transcribed. cDNAs were first amplified for five cycles of annealing at 48°C and then for an additional 30 cycles at 58°C. An aliquot of the reaction was run on a 5% polyacrylamide gel and visualized with ethidium bromide fluorescence. A prominent band was observed at the expected size and was transferred to ZetaProbe membrane. Hybridization of a ^{32}P labeled oligonucleotide probe internal to the PCR primers confirmed that the amplified cDNAs coded for Na channels. The amplified cDNAs were subcloned into M13, plaque purified, and sequenced.

Two genes were isolated from human brain (obtained from autopsy), one gene is most homologous to RBII and the other is most homologous to a rat Na channel gene not previously described. Two genes have been isolated from human muscle biopsies; one (HSM1) is most homologous to rat skeletal muscle I and the second (HSM2) is most homologous to rat skeletal muscle II. HSM2 was obtained only from a patient with a positive diagnosis of skeletal muscle disease. The cardiac cDNAs are presently being sequenced. This method can be used to isolate all human sodium channels and to test the possibility that some diseases are caused by sodium channel defects.

M-AM-J2

GATING CURRENTS OF A SODIUM-CHANNEL MUTANT WITH VERY LOW CONDUCTANCE

Michael Pusch†, Masaharu Noda*, Franco Conti†

(†Istituto di Cibernetica e Biofisica, CNR, I-16146 Genova, *Max-Planck-Institut für Entwicklungsbiologie, D-7400 Tübingen, FRG)

Recently, a TTX-insensitive mutant of the type II Na^+ channel has been described (Noda *et al.*, *FEBS Lett.* **259**: 213-216, 1989). In this mutant, the negative glutamic acid E387 is changed to a glutamine. Motivated by this result, we neutralized the aspartic acid D384 of the sodium channel II, and investigated the properties of the mutant ("D384N") after injecting the corresponding mRNA into *Xenopus* oocytes. In macropatches, upon voltage steps, a relatively small inward current (< 3 pA), and fast, large outward "gating" currents, similar to those of the wild-type could be observed (gating charge up to 15 fC). Substituting various cations (K^+, Li^+, NH^+, Cs^+, TEA^+, Rb^+, Ca^{2+}, Mg^{2+}) for Na^+ did not lead to an appreciable increase of the inward current as compared to the gating current.

1 μM TTX did not eliminate the residual small inward current completely. In solutions with sorbitol as the main constituent, we could record "pure" gating currents in a wide voltage range (-80 to 90 mV). The time course of both the *On* and the *Off* response required the sum of two exponential functions for an adequate fit. The *Off* gating charge showed immobilization of ≈ 70 % at higher voltages. The charge-voltage relationship could be fitted with a Boltzmann distribution, yielding, for one patch, an apparent gating-valence of $z_g = 1.6$ and a mid-voltage of -4 mV.

We conclude, that mutant D384N represents a Na^+ channel with intact gating, but with a highly reduced conductance. The properties of this, and the TTX-resistant mutant E387Q are consistent with the idea that segment SS2, a conserved region between the putative membrane spanning segments S5 and S6 including the residues E387 and D384, participates in the formation of the ion pore.

MP is supported by EEC grant No. SC1*305.

M-AM-J3

A GENETIC DEFECT IN HUMAN SODIUM CHANNELS: EXTERNAL POTASSIUM INDUCES FAILURE OF INACTIVATION S. C. Cannon, R. H. Brown, and D. P. Corey. Dept. of Neurology, Day Neuromuscular Research Center, and Howard Hughes Medical Institute, Massachusetts General Hospital, Boston, MA 02114

Hyperkalemic periodic paralysis (HPP) is a dominantly inherited disorder of episodic weakness, triggered by moderately elevated levels extracellular K^+. We have recently linked HPP to the gene for the α-subunit of the adult muscle sodium channel by RFLP analysis. *In vitro* measurements by others of whole cell currents from muscle biopsies have demonstrated a non-inactivating, tetrodotoxin-sensitive sodium current. To determine the physiologic defect at a single-channel level, we have recorded sodium currents in patches from cultured HPP myotubes. Elevated external K^+ favors an aberrant gating mode characterized by both persistent reopenings and prolonged dwell times in the open state. Panel A shows the superposition of currents measured from 8 depolarizing steps from -80 to -40 mV in an excised patch with 3.5 mM K^+ in the bath. Panel B shows sodium currents recorded from the same patch after the bath was changed to a 10 mM K^+ solution. In patches containing 2 to 5 sodium channels, usually only one channel at a time entered this non-inactivating mode which might persist for up to 10 consecutive depolarizing steps, return to normal inactivation for several steps, then recur. The non-inactivating sodium current was blocked by 100 nM tetrodotoxin. In cell-attached patches containing 0 mM K^+ in the electrode, superfusing the rest of the myotube with 10 mM K^+ after the formation of a gigaohm seal failed to induce the non-inactivating mode. Thus we were unable to detect any evidence of a diffusible intracellular second messenger responsible for this alteration in gating. It is particularly intriguing that a low extracellular concentration of a cation which is abundant intracellularly has such a pronounced effect on sodium channel inactivation - a process largely attributed to an intracellular domain of the sodium channel protein. Large portions of the abnormal gene have been cloned and a sequence analysis of the cDNA may enable us to correlate this abnormal sodium channel function with a localized structural change.

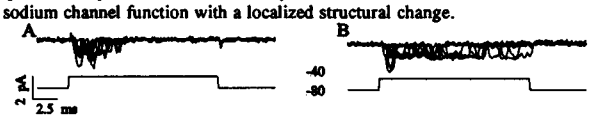

M-AM-J4

BIREFRINGENCE RESPONSES AND GATING CURRENTS ARE ALTERED BY AMILORIDE AND CALMODULIN ANTAGONISTS.

D. Landowne, M. Ichikawa, and G. Matsumoto

University of Miami, Miami, FL
Electrotechnical Laboratory, Tsukuba, Japan.

Internally perfused squid axons were mounted in a polarization microscope. Birefringence responses were measured as changes in light level associated with voltage clamp pulses to 0 mV (ΔBRF-D) and to -140 mV (ΔBRF-H) from a -70 mV holding potential. Gating currents were measured using a P/8 procedure. ΔBRF and gating currents were measured alternately on the same axon.

3mM amiloride in the internal fluid reduced ionic current and ΔBRF-D to about 10% of control. Gating charge was reduced by about 20%. At higher doses ΔBRF-H was also reduced, half-maximal block required 4 mM. The effects were reversible.

Internal perfusion with the calmodulin antagonists, W-5 or W-7, produced similar effects at much lower concentrations. 120 μM W-7 reduced ionic current to one tenth, gating charge by one fifth and ΔBRF-D by three fourths. Half-maximal block of ΔBRF-D was at 45 μM W-7 and 120 μM W-5. The ΔBRF-H was reduced by half with 100 μM W-7 and 200 μM W-5.

Supported by NS26651 and MITI

M-AM-J5

Two components of use-dependent block of Na^+ current by disopyramide and lidocaine in guinea-pig ventricular myocytes

M. HIRAOKA, A. SUNAMI, J. NITTA* AND Z. FAN
Dept. Cardiovasc. Dis., MRI and *2nd Dept. Med.
Tokyo Med. Dent. Univ., Tokyo 113, JAPAN

The mechanism of use-dependent block (UDB) of Na^+ current (I_{Na}) by class I antiarrhythmic agents has not been clarified. We studied the effects of disopyramide (Dis) and lidocaine (Lid) on UDB of I_{Na} in guinea-pig ventricular myocytes. I_{Na} was recorded using the patch clamp technique of whole-cell configuration at room temperature. External Na^+ concentration was reduced to 30 mM with $[Na^+]_i$ = 5 mM. UDB of I_{Na} by 100 uM Dis developed with two exponential time courses in every preparations (n=8). We calculated the degree of UDB, the fast (A_f) and slow (A_s) components of block. In the presence of Dis, degree of UDB, A_f and A_s were not changed at test pulse durations of 20 and 200 msec. Increasing charged form of Dis at pH=8.0, degree of UDB was increased due to increased A_f, while A_s was unchanged. Increasing charged form at pH=6.5, degree of UDB was decreased, leaving only A_s. Therefore, Dis mainly binds to activate state of the Na^+ channel with uncharged form producing A_f and charged form causing A_s. Lid (100 uM) also produced two exponential block developments with pulse durations of 5-200 msec. Prolonged pulse durations or depolarized holding potential increased A_f, whereas increased charged form of Lid at pH=6.5 caused mainly A_s. Internal application of permanently charged lidocaine analogue QX-314 showed a single exponential block development of very slow onset rate. Therefore, uncharged form of Lid binds to inactivated state of the Na^+ channel producing A_f, whereas charged form to activated state causing A_s. These results indicate that charged and uncharged forms of Dis and Lid are responsible for two components of UDB, but their forms are not a sole determinant of the state-dependent binding to the channel.

M-AM-J6

INTERNAL AND EXTERNAL PROTONS MODULATE VOLTAGE DEPENDENCE OF RECOVERY FROM USE-DEPENDENT BLOCK OF LIDOCAINE.

J. Z. Yeh and Joëlle Tanguy. Dept of Pharmacology, Northwestern Univ., Chicago, IL, and MBL, Woods Hole, MA.

Time constants of recovery from use-dependent block of internally applied tertiary amine lidocaine and its quaternary derivative QX-314 were compared at different membrane potentials and different internal and external pHs. At low internal and external pHs, the slow time constant of recovery from use-dependent block (τ_s) by lidocaine was voltage-dependent: τ_s decreased e-fold with a 88 mV and 50 mV hyperpolarization at pH=7.3 and 6.5, respectively. When internal pH was held constant at 7.3, an increase in external pH from 6.5 to 9.0 did not altered the resting block of lidocaine, but reduced use-dependent block by accelerating the recovery time course, decreasing τ_s from 800 ms to about 100 ms at -80 mV. In addition, at external pH > 8 τ_s became voltage independent. When the external pH was held constant at 7.3, an increase in internal pH from 6.5 to 9.0 reduced both resting and use-dependent block, and was almost as effective as external pH change in modulating τ_s. External or internal pH changes did not affect the resting and use-dependent block of QX-314. The magnitude and voltage-dependency of τ_s, which increases e-fold with a 13 mV hyperpolarization, were unaltered. These results with QX314 support the notion that the internal and external pH changes do not affect the drug receptor itself, and suggest that the pathway by which cationic lidocaine escapes from the channel at rest probably differs from that for QX-314. If recovery from lidocaine block at low pH is rate-limited by deprotonation, the voltage dependence of τ_s is not consistent with a simple model in which external H^+ ions can directly titrate the channel-bound drug molecule, because such a model predicts an increase in τ_s with hyperpolarization. Moreover, the effect of internal pH on the voltage-dependency of τ_s is not consistent with a simple titration model involving the internal H^+ ions. The escape of lidocaine molecule from the channel is probably rate-limited by the deprotonation process, which must occur in a more complex manner. (Supported by NIH grant GM 24866).

M-AM-J7

DUAL MECHANISMS OF LOCAL ANESTHETIC INTERACTION WITH SINGLE SODIUM CHANNELS

Kevin J. Gingrich[1], David Beardsley[1], and David T. Yue[2]
[1]Dept. of Anesthesiology, National Naval Medical Center, Bethesda, MD &
[2]Dept. of Biomedical Engineering, Johns Hopkins University, Baltimore, MD

The block of Na currents by local anesthetics (LA) provides important clues about channel architecture, but elementary uncertainties remain as to the molecular mechanism of block. One open question is whether there is a single (Hille, 1977) or multiple (Khodorov et al., 1976) LA binding site(s) within the inner vestibule of the channel. We now find two very different effects of QX-314 (*QX*), a permanently charged LA, upon single cardiac Na channels; so different, in fact, that these effects may correspond to distinct sites. To observe LA action, independent of intrinsic gating, we proteolytically remove fast inactivation by brief exposure of inside-out patches to papain in the bath. Openings then become long-lasting (**A**), but unitary current amplitude (*i*) remains unchanged from before papain exposure (170 mM Na in pipette; isotonic K in bath). Upon bath addition of 2 mM *QX*, two effects are apparent (**B**): *i* is roughly halved at -20 mV and openings are abbreviated by discrete interruptions in current. The fractional reduction in *i* relative to control is markedly enhanced by depolarization, consistent with a binding site deep within the channel (≈ 2/3 of the electrical distance from the inner channel mouth by Woodhull-Hille analysis). In contrast, duration histogram analysis of the discrete interruptions is inconsistent with such a deep-seated site. Open times are shortened by *QX* (6-fold in **A** vs. **B**) in a manner consistent with open channel block; closed times reveal a new slow component with *QX* (12 ms in **B**). Block and unblock rates derived from these were little affected by voltage, suggesting that the site of interaction associated with discrete block resides considerably closer to the cytoplasmic end of the channel. Beyond the question of binding site numerology, features of the discrete block provide new insight into how *QX* might work when fast inactivation is present. The mean time to first opening is strikingly slowed by *QX* (11-fold in **A** vs. **B**, depolarization at arrow), arguing that either *QX* can be tightly trapped in the channel upon repolarization, or that closed channels can be blocked appreciably by *QX*. The former possibility is inconsistent with the absence of use-dependence after proteolytic removal of inactivation; thus, we argue that closed channels can be blocked directly by *QX*, in contradiction with the guarded-receptor hypothesis. The key feature of depolarization that leads to use-dependence may not be to make available open channels that are much more readily blocked than closed channels, but to cause the inactivation "ball" to trap and stabilize *QX* bound to either open or closed channels.

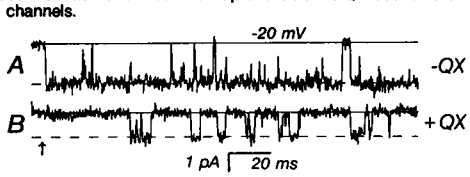

M-AM-J8

PROTON PERMEATION THROUGH CARDIAC SODIUM CHANNELS

Peter H. Backx and David T. Yue, Dept. of Biomedical Engineering, Johns Hopkins University, Baltimore, MD

Proton mobility in H_2O is uniquely high due to "charge relay" effects. As such, proton block and permeation of ionic channels are especially interesting since even a single file of H_2O lining the permeation pore would result in a high permeability of protons, as in gramicidin. In Na^+ channels, however, the mechanism of the reduction in whole cell currents by protons (H^+) remains unclear. Although intrapore blocking by H^+ has been considered (Woodhull, J Gen Phys, 1973), surface charge effects may also account for much of this reduction. We have re-examined the underlying mechanism of Na^+ current block in single Na^+ channels modified by the addition of fenvalerate (2-10μM) which removed fast inactivation and reduced channel closure due to deactivation, even at very negative voltages. Using inside-out patches we were thereby able to examine the voltage dependence of proton block over the voltage range from -180mV to 120mV with symmetric $[Na^+]$. Under control conditions (Bath (mM): 140 Na^+, 10 Hepes, pH 7.4. Pipette (mM): 140 Na^+, 10 Hepes, 0.5mM Ba^{2+}), the I-V relationship was linear between 60mV and -60mV (slope = 32pS), but flattened out at more positive and negative voltages. With pH=5.5 in the pipette, the unitary conductance of the Na^+ was reduced at all voltage studied (-180mV to 120mV). (Compare raw traces at pH = 5.5 and 7.4, filtered at 1kHz). Furthermore the ratio of the currents ($I_{5.5}/I_{7.4}$) showed a parabolic dependence (See figure) on voltage. At voltages above -50mV the ratio of the currents increased monotonically with voltage. Interestingly, at more negative voltages (ie < -90mV) the ratio turned sharply upward in a much more pronounced manner than previously observed in squid axons (Begenisich and Danko, J Gen Phys, 1983). This upturn at negative voltages cannot be explained by a reduction of surface charges by H^+, but instead suggests that protons actually permeate the Na^+ channel at very negative voltages. In fact, based on fits to a single intrapore binding site model to our data, we estimate that protons bind to a site located at an electrical distance of about 0.25 while en route through the channel.

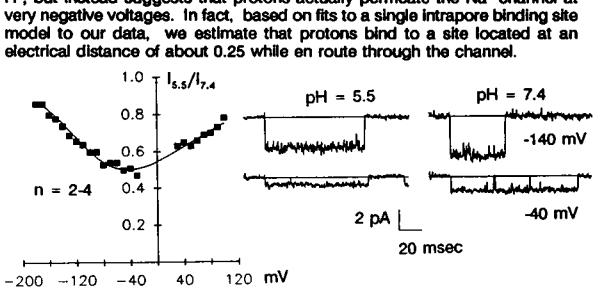

M-AM-K1

NEUROTENSIN-ACTIVATED Cl^- CURRENTS IN HT29 CELLS. G.E. Breitwieser* and M.H.Montrose#. Depts. of Physiology*# and Medicine#, Johns Hopkins University School of Medicine, 725 N. Wolfe Street, Baltimore, MD 21205.
Neurotensin-activated Cl^- currents were studied by the whole cell patch clamp technique in cultured HT29 cells. Bath addition of 100 nM neurotensin resulted in the activation of two distinct currents, an "early" current, whose onset and duration correlates with the neurotensin-induced release of intracellular Ca^{++}, and a "late" Cl^- current which rectifies in symmetrical Cl^- solutions and begins to activate within 30 sec of neurotensin addition. The "early" current duration can be increased by inclusion of 50 μM IP_3 in the pipet solution, confirming its dependence on intracellular Ca^{++}. The "late" current corresponds to a rectifying Cl^- current which can also be activated by bath application of either 100 μM dibutyryl-cAMP or 1-5 μM ionomycin. Activation of the "late" current can be blocked by a variety of protein kinase inhibitors, including W13 and H7. Neurotensin activation of the "late" current prevents further activation of current by either dibutyryl-cAMP or ionomycin, suggesting that all three agents activate the same class of channels. Activation of the "late", presumably phosphorylated, current does not decay on removal of neurotensin from the bath, suggesting the possibility of a receptor-mediated inactivation pathway. HT29 cells thus represent a model system in which to study the convergence of distinct signal transduction pathways on a single class of Cl^- channel. Supported by NIH, CFF and AHA.

M-AM-K2

Ca^{++}/CALMODULIN-DEPENDENT PROTEIN KINASE II (CaMKII) MEDIATES STIMULATION OF Cl^- CONDUCTANCE BY Ca^{++} IN EPITHELIAL CELLS. Roger T. Worrell & Raymond A. Frizzell Dept. Physiology & Biophysics, Univ. of Alabama at Birmingham, Birmingham, AL 35294.

Separate Ca^{++}-, cAMP-, and volume-sensitive Cl^- conductances have been identified in epithelial cells using the whole-cell patch clamp technique. We used the colonic secretory cell line, T84, to study the mechanism whereby increased cytosolic Ca^{++}-leads to increased Cl^- conductance. Basal current levels, using symmetrical NMDG-Cl bath and pipette solutions, were typically low (-50pA) and increased to 1.1±0.2(n=10) nA/20pF (at +100mV) on exposure to 2μM ionomycin. Bath application of the calmodulin antagonists (50μM) trifluoperazine, calmidazolium, or sphingosine reversibly inhibited the Ca^{++}-stimulated whole-cell Cl^- conductance to basal levels. This suggests that Ca^{++} acts through calmodulin to stimulate Cl^- conductance rather than acting directly on Cl^- channels. The protein kinase C antagonists, H7 and phloretin (50μM), had no effect on conductance development in response to Ca^{++}. To determine the possible involvement of protein kinases in the Ca^{++}-dependent stimulation of Cl^- conductance we employed specific pseudosubstrate peptide inhibitors of PKA, PKC, and CaMKII. Cellular concentrations of inhibitors were estimated to be 10-20 times the K_i values for kinase inhibition *in vitro*. No effect on the development of Ca^{++}-stimulated Cl^- conductance was observed with pipette solutions containing the PKA peptide inhibitor, PKI (115nM), or the PKC inhibitor, PKC(19-36) (7.5μM). In contrast, Ca^{++}-stimulated Cl^- conductance development was abolished with pipette solutions containing 10μM of the CaMKII peptide inhibitor, CaMKII(273-302). The truncated control peptide, CaMKII(284-302) (20μM), did not affect current development. These data suggest that calmodulin, acting through the Ca^{++}/calmodulin-dependent kinase II, mediates the Ca^{++}-stimulation of Cl^- conductance in colonic secretory cells. [Supported by NIH DK31091 and the Cystic Fibrosis Fdn].

M-AM-K3

PROTEIN KINASE C (PKC) AND ARACHIDONIC ACID (AA) INHIBIT THE APICAL SMALL-CONDUCTANCE K^+ CHANNEL OF RAT CORTICAL COLLECTING DUCT (CCD). Wenhui Wang and Gerhard Giebisch. Department of Cellular. and Molecular Physiology, SHM, Yale University, New Haven, CT 06510

The small-conductance K^+ channel with inward slope conductance of 35 pS and outward slope conductance of 15 pS is a main contributor to the apical K conductance of rat CCD and responsible for K^+ secretion in this segment. The channel is sensitive to pH, ATP and the ATP/ADP ratio(Am. J. Physiol. 259:F494-F502, 1990). In the present study we have further investigated the modulatory effect of PKC and AA on the apical small-conductance K^+ channel of principal cells of rat CCDs using the patch-clamp technique at 37°C. To study cell-attached patches, tubules were superfused with (in mM) 140 NaCl, 5 KCl, 1.8 $MgCl_2$, 1.8 $CaCl_2$ and 10 Hepes (pH 7.4). The Ca^{2+} concentration of the bath in inside-out patches was reduced with 1 mM EGTA to 10 nM, 100 nM or 1 μM. In cell-attached patches (140 KCl in the pipette) addition of 10 μM PMA (phorbol 12-myristate 13-acetate) to the bath reduced channel open probability (P_o) and current amplitude progressively within 6-10 minutes. In inside-out patches 1 unit/ml PKC in the presence of 1 μM OAG (1-oleoyl-2-acetyl-sn-glycerol) and 0.1 mM ATP reduced the P_o of the channel, and the PKC-induced decrease of P_o was dependent on the free Ca^{2+} concentration (11% in 10 nM; 23% in 100 nM and 42% in 1 μM free Ca^{2+}, respectively). The channel is also blocked by application of 25-50 μM AA in the bath which progressively inhibited and eventually closed the channel of inside-out patches. The effects of PKA and PKC on channel activity are reversible. The results indicate that PKC and AA are both important modulators of the gating mechanism of the secretory K^+ channel.

M-AM-K4

WHOLE-CELL K^+ CURRENTS IN ISOLATED FROG SKIN EPITHELIAL CELLS. J. Fernando Garcia-Diaz, Dept. Physiology, Boston University School of Medicine, Boston, MA 02118.

Whole-cell currents were studied in cells from frog (*R. pipiens* and *R. catesbiana*) skin, isolated by collagenase and trypsin treatment and kept in primary cultures up to 3 days. Patch pipettes contained 117 mM K, 24 mM Cl, ATP and EGTA. Access to the cell interior was gained either through a combination of suction and voltage pulses or by the inclusion of nystatin in the pipette solution. Currents were elicited by voltage steps of 200 ms from a holding potential of -60 mV. Since currents were not time dependent, they were subsequently evoked by applying a voltage ramp of 100 mV/s from -160 mV to 100 mV. With an external K gluconate Ringer solution the currents showed slight inward rectification reversing at 10±5 mV (n=19) and with a conductance of 5±3 nS at the reversal potential. Substitution of Na or NMDG for K in the bath reduced cell conductance to the same extent and shifted the reversal potential to negative values. Addition of amiloride (20 μM) to the Na gluconate solution had no effects. These results show that most of the cell conductance is due to K with little or no Na conductance present, confirming that most cells originate from deeper epithelial layers and contain membranes with basolateral properties. Outward currents were also smaller with Na or NMDG in the medium than with K, resulting in crossover at positive voltages. This indicates a stimulation of K efflux by external K and suggests a multi-ion transport mechanism. The current was reversibly inhibited by external Ba (5 mM) and quinidine (0.1-1 mM). Blockade by Ba was strongly voltage-dependent while that by quinidine was not. Similarities in IV relations and blockage suggest that the currents are sustained by an inward rectifier K channel previously described in this preparation (Biophys.J.*57*:84a, 1990). This channel is likely responsible for the basolateral K conductance in the intact epithelium. Supported by USPHS DK 39214.

M-AM-K5

DIFFERENTIAL INHIBITION OF WATER AND UREA PERMEABILITIES IN ISOLATED PROXIMAL TUBULE CELLS FROM THE RABBIT KIDNEY. M. Echevarría, A. Gutierrez, F. González and G. Whittembury, Instituto Venezolano de Investigaciones Científicas (IVIC) and E. Medicina J.M. Vargas, Caracas, Venezuela.

Diffusive water (Pw) and urea (Pu) permeabilities were calculated in isolated proximal tubule cells from the linear diffusion of THO and 14-C urea in a packed cell column (Kidney Int 30:187, 1986; J. Mem. Biol. 104:35, 1988; Proc. IUPS 17:496, 1989; AJP 251:C872, 1986). At 14°C Pw and Pu were 66 ± 8 and 18 ± 3 μm/s. Preincubation for 20 min in pCMBS 0.2 mM has no effect on Pw but it inhibits Pu. pCMBS 2 mM markedly inhibits Pw and Pu. Addition of 5 mM DTT reverted the action of pCMBS. Phloretin 0.6 mM strongly inhibited Pu but did not affect Pw. Similarly KMnO4 30 μM did not affect Pw but markedly inhibited Pu. The energy of activation for Pw was ∿2 and Pu was ∿7 kcal/mole. This different behaviour of Pw and Pu in the presence of different agents indicates that they do not share the same permeation pathway. It is concluded that water and urea proteinic permeation pathways are different. The dose-dependent inhibition of Pw and Pos (the water osmotic permeability) by pCMBS allows to calculate a dPos/dPw of 15. This indicates that water uses single file channels with ∿15 water molecules/channel. The equivalent radius of these channels must be> 1.5 (the molecular radius of water) and < 2.3 A (the molecular radius of urea) so that water can flow through but the urea molecule is excluded from them. The water channels close when their sulfhydryl groups are oxidized (pCMBS). They remain open when they are reduced (control, DTT). From the values of Pd, Pu, the K permeability and single channel K conductance it may be calculated there are 10,000 - 100,000 water channels, 1.000 urea channels and 1 K channel per μm^2 of cell surface.

M-AM-K6

FREQUENCY-DEPENDENT COMPLEX DIELECTRIC PROPERTIES OF AN EPITHELIAL PLASMA MEMBRANE. Mouhamed S. Awayda, Willy Van Driessche, and Sandy I. Helman. Univ. of Illinois, Urbana, IL 61801

Voltage clamp electrical impedance analysis was done to determine the frequency dependence of apical membrane capacitance (C_a) of intact and isolated epithelia of frog skin (R. pipiens). Sulfate Ringer-bathed tissues were short-circuited and studied at 25° and 33°C while exposed to 100 μM amiloride and a Na-free (NMDG) apical Ringer solution to cause $Z_a >>> Z_b$. Shunt resistance ranged between 6 and 75 $K\Omega \cdot cm^2$. C_a determined at 106 discrete frequencies between 0.1 Hz and 5.5 KHz showed frequency dependence in agreement with previous and present observations of depressed semi-circles of Nyquist impedance plots. Complex plane plots of real and imaginary components of C_a indicated the existence of two major relaxation processes at characteristic frequencies near 1 Hz and near a few hundred Hz that are temperature-dependent. Magnitude and phase [Magnitude/degrees] of C_a at 1, 10, 100, and 1000 Hz averaged 2.35/-3.3, 2.12/-5.8, 1.67/-11.2, and 1.23/-10.6 $\mu F/cm^2$ respectively which remained essentially constant for 60 minutes following inhibition of Na transport by amiloride + O[Na]. A 2.5 μM forskolin-mediated increase of intracellular cAMP caused, after a delay of 2 to 3 minutes, a gradual increase of C_a to 119.6 ± 2.7% above control at 30 min, following a time course similar to the increase of apical membrane Na channel density observed previously (Els and Helman). Similar increases of C_a were observed at all frequencies indicating increase of membrane area. We conclude 1) that frequency-dependence of the membrane dielectric is due to existence of audio and sub-audio relaxation processes and 2) that apical membrane area is dependent upon intracellular cAMP. (Supported by NIH DK30824.)

M-AM-K7

GASTRIC ACID IS SECRETED FROM A PREFORMED ACID POOL. Vojtech Licko and E.B. Margareta Ekblad, Cardiovascular Research Institute, University of California, San Francisco CA 94143

Continuous monitoring of frog gastric acid secretion by flow-through Ussing chambers/pH-stat methodology discloses steps involved in the secretory processes inaccessible to direct detection. The use of conservative inhibitors resulting in no net loss of acid after the inhibitor removal due to a rebound phenomenon as opposed to the effect of the non-conservative inhibitors, led to a two-step hypothesis: the acid formation and the proton translocation are two distinct processes. To argue quantitatively, a mathematical model based on observations with stimulants and both kind of inhibitors was constructed, identified and tested. The principal features of the model are those of an open system with saturable metabolic rate. The stimulants increase the rate of acid formation via receptor-binding mediated process which is competitively inhibitable by a histamine antagonist (metiamide) whose effect is, therefore, nonconservative. A conservative inhibitor, e.g., nitrite, competitively inhibits the proton translocation and, therefore, has a conservative effect. Thus, the model's compatibility with the data vindicates the validity of the two-step hypothesis in contraposition to the current belief which holds that free protons are liberated from their precursorial form on the plasma membrane and concurrently released to the extracellular space.

M-AM-K8

ION TRANSPORT IN MAMMALIAN TASTE CELLS: RESULTS FROM COMPUTER SIMULATION. Sheella Mierson (University of Delaware, School of Life & Health Sciences, Newark, DE 19716, U.S.A.)

The sensation of taste is mediated by electrical events in taste bud cells, which are embedded in the tongue epithelium. A model, based on network thermodynamics and consistent with usual epithelial topology, was developed for the rat tongue epithelium (M.L.Fidelman & S.Mierson., *Am.J.Physiol.*, *257*:G475-G487, 1989). The model includes amiloride-sensitive Na^+ channels in the apical membrane, and K^+ channels and Na^+-K^+ pumps in the basolateral membrane. The model successfully simulates some aspects of both steady-state and transient electrical measurements observed in the rat tongue when exposed to a wide range (50-2000 mM) of NaCl concentrations, the concentration range of interest for gustation. The simulations lead to two main results: (1) In a time-dependent analysis, in response to a prolonged hyperosmotic NaCl stimulus, the model predicts intracellular depolarization followed by repolarization. Since the intracellular potential has been identified with the taste receptor potential, the depolarization and subsequent repolarization may explain the phenomenon of adaptation, in which the taste nerve signal shows a rapid initial increase followed by a decrease when the tissue is exposed to a hyperosmotic salt stimulus. The calculated sequence of depolarization and repolarization is due to the organization of the component membranes and cannot be predicted from properties of the individual membranes in isolation. (2) Steady-state calculations indicate that the Na^+ channel in the luminal membrane of the taste cell must have different properties than those typical in other tight epithelia. An equation for a one-site, two-barrier channel is used to describe the apical Na^+ channel (E.Mintz, S.R.Thomas, & D.C.Mikulecky, *J.Theor. Biol.*, *123*:21-34, 1986). In order for the taste cell to depolarize as the salt concentration increases, the equilibrium dissociation constant for the Na^+ binding site must be an order of magnitude higher than the usual value. Both these results suggest experiments for confirmation. This work supported by NSF Grant BNS-8819253.